Of mice and humans: de Jong and Maina provide an overview of the positive aspects as well as the shortcomings of laboratory animals as translational models for human studies, with a focus on tumor scintigraphy and radionuclide therapy. . . . . **Page 501**

Myocardial viability assessment: Allman offers perspective on the history and status of ^{18}F-FDG PET viability imaging in directing management of patients with coronary artery disease and poor left ventricular function and previews a related study in this issue of *JNM*. . . . **Page 505**

Bowel prep and PET/CT: Soyka and colleagues investigate the usefulness of bowel preparation before ^{18}F-FDG PET/CT imaging to reduce physiologic intestinal uptake. . . . . **Page 507**

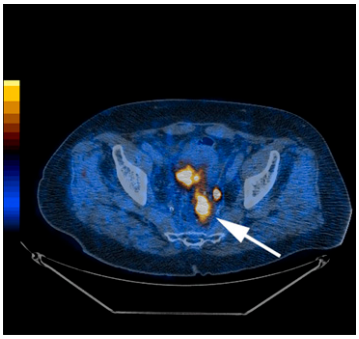

PET in schizophrenia: Patel and colleagues review the use of PET tracers and kinetic modeling in identifying regional brain abnormalities associated with cognitive functioning in schizophrenia, including challenges and future investigational directions in dopaminergic function. . **Page 511**

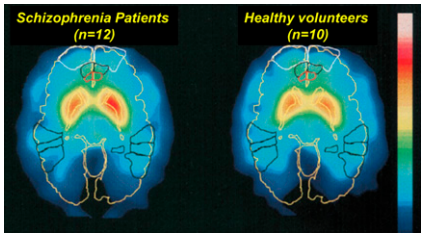

PET and breast cancer metastases: Doot and colleagues evaluate the accuracy of ^{18}F-fluoride model parameter estimates for characterizing regional kinetics in metastases and normal bone in breast cancer patients, with implications for PET assessment of bone turnover during therapy. . . . . **Page 521**

PET/CT and tumor cell proliferation: Yue and colleagues determine whether serial ^{18}F-FLT uptake on PET/CT can monitor the biologic response of esophageal squamous cell carcinoma and normal tissues to radiotherapy. . . . . **Page 528**

Dual-phase PET in lung adenocarcinoma: Houseni and colleagues investigate the prognostic value of glucose metabolism dynamics as assessed by dual-phase ^{18}F-FDG PET in patients with adenocarcinoma of the lung. . . . . **Page 535**

PET, breast cancer, and molecular markers: Osborne and colleagues explore the relationship between specific markers (estrogen and progesterone receptors and *HER2* status) and tumor glucose use as measured by PET in patients with breast cancer. . . . . **Page 543**

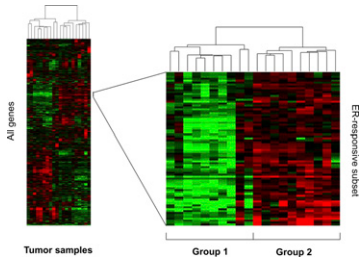

PET monitoring in sarcomas: Dimitrakopoulou-Strauss and colleagues evaluate the effect of early dynamic ^{18}F-FDG PET imaging on management and outcomes in patients with soft-tissue sarcomas who received neoadjuvant chemotherapy. . . . . **Page 551**

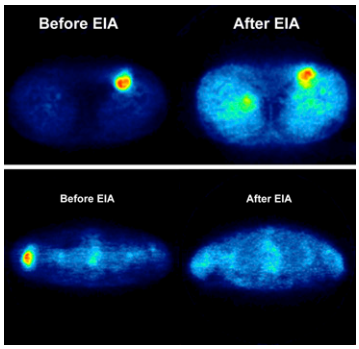

Quantifying P-gp function: Kreisl and colleagues look at the ability of ^{11}C-dLop PET to quantify permeability-glycoprotein function at the blood–brain barrier in humans. . **Page 559**

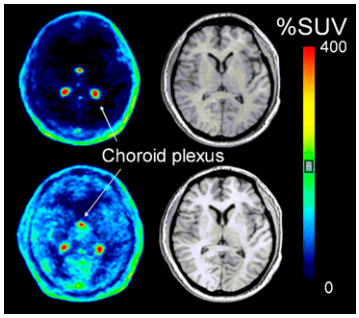

PET in viability evaluation: Abraham and colleagues from the PET and Recovery Following Revascularization (PARR 2) study report on a subanalysis of PET cardiac management in a center with experience, ready access to ^{18}F-FDG, and integration with clinical teams. . . . . **Page 567**

Reducing artifacts in cardiac PET/CT: Lubberink and colleagues assess the accuracy of myocardial blood flow and coronary flow reserve measurement by ^{15}O-water PET in the absence of attenuation correction. . . . . **Page 575**

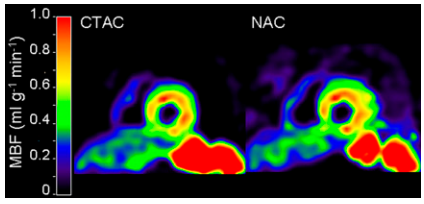

^{18}F-DMFP PET and parkinsonian syndromes: la Fougère and colleagues describe the utility of the selective dopamine receptor ligand ^{18}F-desmethoxyfallypride for differential PET diagnosis of patients with idiopathic and nonidiopathic parkinsonian syndromes. . . . . **Page 581**

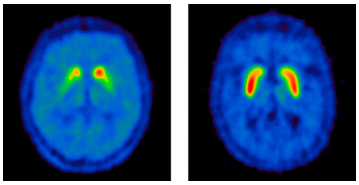

^{11}C-raclopride PET and parkinsonism: Van Laere and colleagues explore potential improvements in ^{11}C-raclopride PET differentiation between Parkinson disease and multiple-system atrophy with predominant parkinsonism through addition of dynamic scan analysis combining striatal dopamine-2 binding and regional tracer influx. . . . . **Page 588**

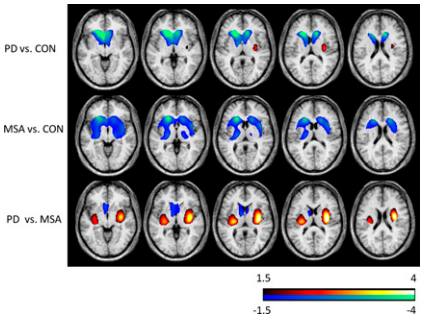

Imaging approaches to Parkinson disease: Brooks provides an educational overview of the current roles of structural and functional imaging for diagnosing and managing different parkinsonian syndromes. . . **Page 596**

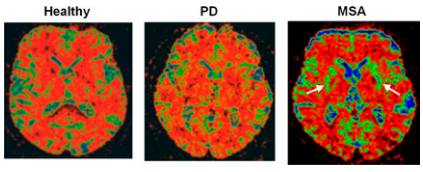

Positron emitters and small-animal PET: Disselhorst and colleagues report on detailed image quality assessments for several positron emitters using national standards in a high-resolution small-animal PET lutetium-oxyorthosilicate scanner. . . . . **Page 610**

Vitamin C and salivary ^{131}I dosimetry: Liu and colleagues investigate the effect of vitamin C administered at various times on salivary absorbed dose of therapeutic radioiodine in patients with differentiated thyroid cancer. . . . . **Page 618**

Antiangiogenic agents and RIT efficacy: Kraeber-Bodéré and colleagues evaluate the results of combining anti–carcinoembryonic antigen ^{131}I-F6 monoclonal antibody radioimmunotherapy with thalidomide or a cyclopeptic vascular endothelial growth inhibitor in a mouse model of thyroid cancer. . . . . **Page 624**

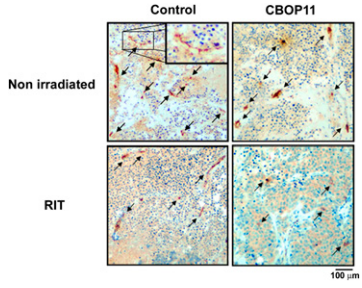

^{18}F-FDG uptake in micrometastases: Li and colleagues examine ^{18}F-FDG uptake in microscopic tumors grown intraperitoneally in mice and relate this to physiologic hypoxia and glucose transporter-1 expression. . . **Page 632**

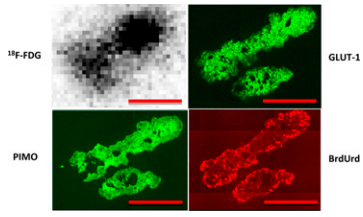

^{68}Ga-siderophores for PET: Petrik and colleagues evaluate the potential of radiolabeled iron-complexing ferric ion siderophobes in PET diagnosis of invasive pulmonary aspergillosis. . . . . **Page 639**

Gated PET of regional lung volume change: Wellman and colleagues present a method using respiratory-gated PET images of inhaled ^{13}N-nitrogen to measure regional specific lung volume change, a key variable in lung mechanics and pathogenesis of ventilator-induced lung injury. . . . . **Page 646**

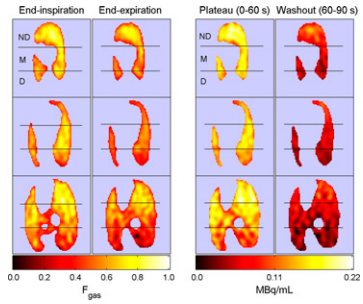

3D-based patient-specific dosimetry: Amro and colleagues describe the development of a 3-dimensional imaging–based dosimetry methodology incorporating antitumor biologic effects with biologically effective dose and equivalent uniform dose and present an example in patients with non-Hodgkin lymphoma undergoing radioimmunotherapy. . . **Page 654**

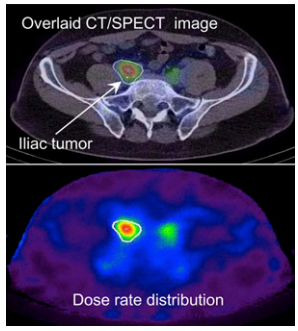

ON THE COVER

^{18}F-FLT uptake can be used to monitor the biologic response of esophageal squamous cell carcinoma to radiotherapy and may have an advantage over ^{18}F-FDG in differentiating inflammation from tumor. Increased uptake of ^{18}F-FLT after treatment interruption, as occurred in the patient shown here, may reflect accelerated repopulation. After the interruption, tumoral uptake rose above baseline whereas uptake in irradiated bone marrow decreased.

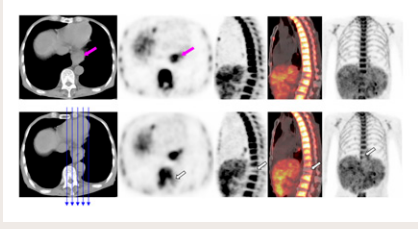

See page 532.